Journal of Engineering Mathematics **38:** 297–308, 2000.

Modeling of textile composites with warp/weft frictional contact

J. KOKO
ISIMA, Université Clermont-Ferrand II Campus des Cézeaux - BP 125, 63173 Aubière cedex, France

Received 27 October 1997; accepted in revised form 23 December 1999

Abstract. A 2D modeling of textile composites is studied. The modeling is applicable to woven textile composites with flat fibers, used as reinforcing fibers of composite materials. Two 2D displacement fields are introduced, one for each layer of the fabric. The warp/weft interaction is taken into account by a nonlinear functional which characterizes the frictional contact. An explicit form of the warp/weft contact pressure is proposed. A numerical approximation of a solution of the variational problem is presented.

Key words: textile composites, Coulomb friction, variational inequalities

1. Introduction

We study the two-dimensional behavior of textile composites used as reinforcing fibers of composite materials. The modeling is applicable to textile composites with flat fibers, made from glass, carbon, kevlar, ... for which the warp/weft contact area is significant. The model is two dimensional because the constitutive equations are set in the plane and displacement fields considered are two-dimensional.

There exist various mechanical models for textile composites [1], but most of them do not express explicitly the warp/weft interaction within the textile composite plate. These models are generally suitable for coated textile composites. For uncoated textile composites, Caillerie and Tollenaère [2] propose a 2D model with a warp/weft linear elastic spring back. Following Leguillon and Lené [3], they use two 2D displacement fields, one for each layer of the textile composite plate. But due to the frictional contact, the warp/weft interaction is neither linear nor elastic.

In this paper we keep the two-layers model of Caillerie and Tollenaère [2]. We replace the linear elastic spring back by a warp/weft frictional contact term. Our motivation for this study lies in an attempt to model the forming (or draping) of textile composites, which is necessary for composite materials with complex geometries. Certain properties of the final component, such as stiffness, thermal expansion or conductivity are dependent on the reinforcing fibers location within the component. The 2D model presented here can be regarded as a first step towards this goal. Note that there exist numerical simulation methods, for draping of textile composites, based on *geometric assumptions* (Bendali *et al.* [4], Van West *et al.* [5]) without mechanical properties of the fabric.

The paper is organized as follows. In Section 2 we state the mechanical problem with frictional contact, under the small deformations assumption. In Section 3 we give an explicit expression for the warp/weft contact pressure. A variational formulation is given in Section 4. In Section 5, we discuss the numerical approximation of a solution of the problem.

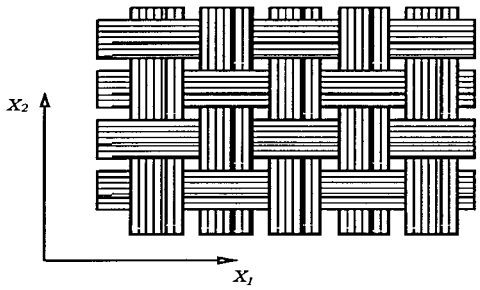

Figure 1. Detail of a woven textile composite plate.

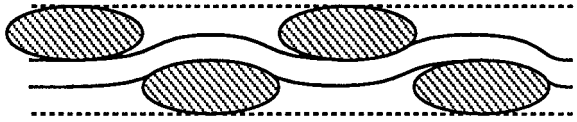

Figure 2. Cross-section of the fabric.

2. Modeling of the warp and weft layers

We consider the woven textile composite plate represented in Figure 1, which occupies a domain Ω in $\mathbb{R}^2$ of boundary $\Gamma = \partial\Omega$. The plate consists of two families of fibers : warp fibers (parallel to x_2-axis) and weft fibers (parallel to x_1-axis).

The idea, due to Caillerie and Tollenaere [2], consists of considering each family of fibers as a separate *continuous layer*. Then we need two displacement fields u^α, for $\alpha = 1, 2$; with $u^\alpha = (u_1^\alpha, u_2^\alpha)$ the in-plane displacement field of the layer α. We set $\mathbf{u} = (u^1, u^2)$, the displacement field of the plate. Under the small deformations assumption, constitutive equations for each layer α are (repeated-index convention)

$$\sigma_{ij}^\alpha = a_{ijkl}^\alpha \mathcal{E}_{kl}(u^\alpha), \quad i, j, = 1, 2 \tag{1}$$

$$\mathcal{E}_{kl}(u^\alpha) = (\partial_l u_k^\alpha + \partial_k u_l^\alpha)/2, \quad k, l = 1, 2. \tag{2}$$

The elasticity constants a_{ijkl}^α of the layer α are generally obtained by homogenization. As shown in Figure 2, the weaving creates a fibers waviness. Then elasticity constants a_{ijkl}^α must take into account the reduction due to the fibers waviness. We use here a simple rule due to Cox and Dadkhah [6] (see also [1]) for computing a_{ijkl}^α.

Let E^α and G^α be the axial and shear moduli of a fiber and ν^α is its axial Poisson's ratio. Suppose that the waviness takes the form of sinusoidal oscillations in the path of a fiber, with a wavelength l^α and an amplitude d^α, α being the number of the layer. Cox and Dadkhah [6] show that the stiffness of a layer is reduced by the factor

$$\kappa^\alpha = \left\{1 + \pi^2 \left(\frac{d^\alpha}{l^\alpha}\right)\left[\frac{E^\alpha}{G^\alpha} - 2(1 + \nu^\alpha)\right]\right\}^{-1}, \quad \alpha = 1, 2. \tag{3}$$

Let $\tilde{a}_{ijkl}^\alpha$ be the homogenized elasticity constants of a layer α, formed of *straight fibers*. The elastic-moduli tensor $(\tilde{a}_{ijkl}^\alpha)$ is obtained by classical homogenization methods, see for example Caillerie and Tollenaère [2]. Then the elastic-moduli tensor of a layer α of the plate is given by

$$a^{\alpha}_{ijkl} = \kappa^{\alpha}\tilde{a}^{\alpha}_{ijkl}. \tag{4}$$

We assume that the plate is fixed on a part of its boundary $\Gamma_0 = \Gamma_0^1 \cup \Gamma_0^2$, with $\text{mes}(\Gamma_0^\alpha) > 0$. The plate is subjected to in-body forces f^α. Equilibrium equations of layers are (without any consideration on warp/weft interaction)

$$\text{div}\sigma^\alpha + f^\alpha = 0 \quad \text{on } \Omega^\alpha, \alpha = 1, 2, \tag{5}$$

$$u^\alpha = 0, \quad \text{on } \Gamma_0^\alpha, \alpha = 1, 2. \tag{6}$$

It remains to introduce the warp/weft frictional contact. Let $p(\mathbf{u}) > 0$ be the (unknown) warp/weft contact pressure, which depends on the solution $\mathbf{u} = (u^1, u^2)$ of the problem. Let $\mu_F > 0$ be the friction coefficient. The tangential relative displacement is $\bar{\mathbf{u}} = u^1 - u^2$. If σ_T is the tangential stress then the warp/weft frictional contact condition can be written as (Coulomb law)

$$|\sigma_T(\mathbf{u})| < \mu_F p(\mathbf{u}) \Rightarrow \bar{\mathbf{u}} = 0, \tag{7}$$

$$|\sigma_T(\mathbf{u})| = \mu_F p(\mathbf{u}) \Rightarrow \exists\gamma > 0, \text{ such that } \bar{\mathbf{u}} = -\gamma\sigma_T(\mathbf{u}). \tag{8}$$

In the next section, we give an explicit formula for the warp/weft contact pressure $p(\mathbf{u})$.

3. Modeling of the warp/weft frictional contact

As shown in Figure 2, the weaving introduces a waviness of fibers. Since most of the fibers used have a high elastic modulus, a stretch λ^α of a fiber of a layer α implies lower (if $\lambda^\alpha \leq 1$) or higher (if $\lambda^\alpha > 1$) contact pressure on the other layer. The warp/weft contact pressure can therefore be considered as a function of the stretch of fibers of the plate.

Let $\eta > 0$ be the initial warp/weft contact pressure due to weaving. Since the textile composite is a periodic structure, η is a mean-value on a unit cell. Let p^α be the contact pressure produced by the layer α. We assume that the contact pressure is a *linear function of the stretch, i.e.*

$$p^\alpha = \eta\lambda^\alpha/2, \quad \alpha = 1, 2. \tag{9}$$

Then the warp/weft contact pressure, within the plate, is

$$p = p^1 + p^2 = \eta(\lambda^1 + \lambda^2)/2. \tag{10}$$

Note that if $\lambda^1 = \lambda^2 = 1$, then $p = \eta$ the initial warp/weft contact pressure.

Let $\mathbf{e_1}$ and $\mathbf{e_2}$ be natural base vectors of $\mathbb{R}^2$. Then stretch functions λ^α are given by (no summation over α)

$$\lambda^\alpha(u^\alpha) = |\mathbf{e}_\alpha + \partial_\alpha u^\alpha|, \quad \alpha = 1, 2 \tag{11}$$

where $|\cdot|$ is the Euclidean norm of $\mathbb{R}$. Unfortunately, the stretch function given by (11) leads to mathematical difficulties with the friction functional. Since we work under the small-deformations assumption, we can neglect nonlinear terms under the square root in (11). Then, using the approximate formula $\sqrt{1+\varepsilon} \approx 1 + \varepsilon/2$, we obtain the linearized stretch function (no summation over α)

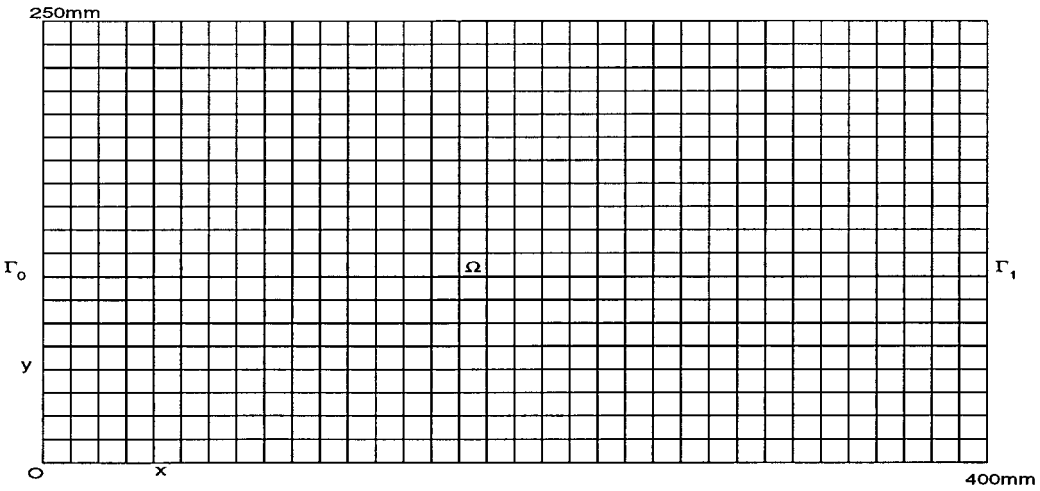

Figure 3. Finite elements mesh of the plate in its undeformed configuration.

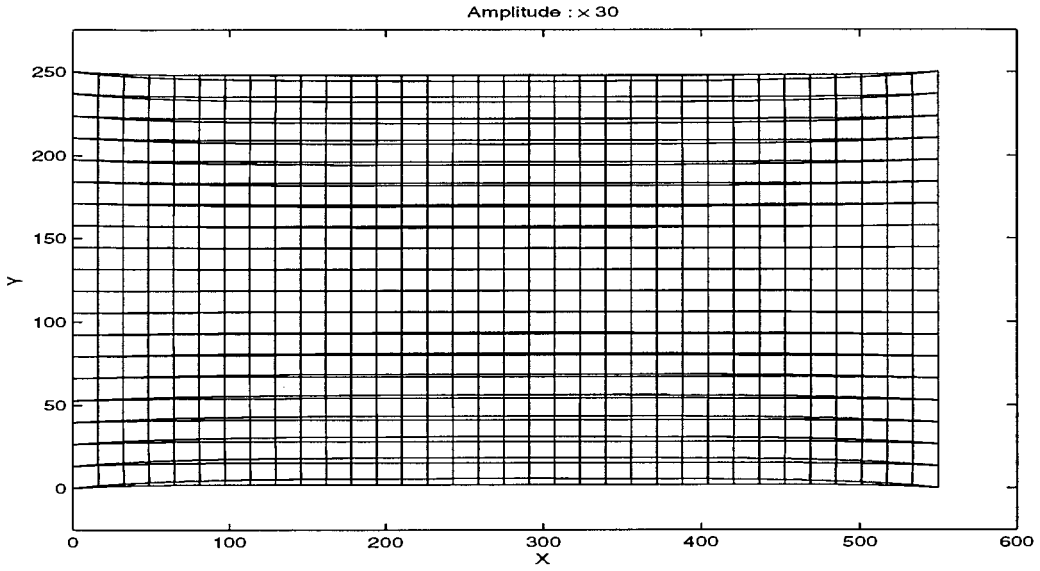

Figure 4. Deformed configuration of the plate Ω subjected to the prescribed displacement $u^{\alpha}_{\Gamma_1} = 5\mathbf{e_1}$ mm.

$$\lambda^{\alpha}(u^{\alpha}) = 1 + \partial_{\alpha} u^{\alpha}_{\alpha} = 1 + \mathcal{E}_{\alpha\alpha}(u^{\alpha}), \quad \alpha = 1, 2. \tag{12}$$

Substituting (12) in (9), we find that the warp/weft contact pressure is

$$p(\mathbf{u}) = p^1(u^1) + p^2(u^2) = \frac{\eta}{2}(2 + \mathcal{E}_{11}(u^1) + \mathcal{E}_{22}(u^2)). \tag{13}$$

4. Variational formulation

In order to derive variational formulation of the problem (5) - (8), we begin by defining spaces, set and forms used. We set

$$\mathbf{L^2}(\Omega) = (L^2(\Omega))^4 \quad \text{and} \quad \mathbf{H^1}(\Omega) = (H^1(\Omega))^4.$$

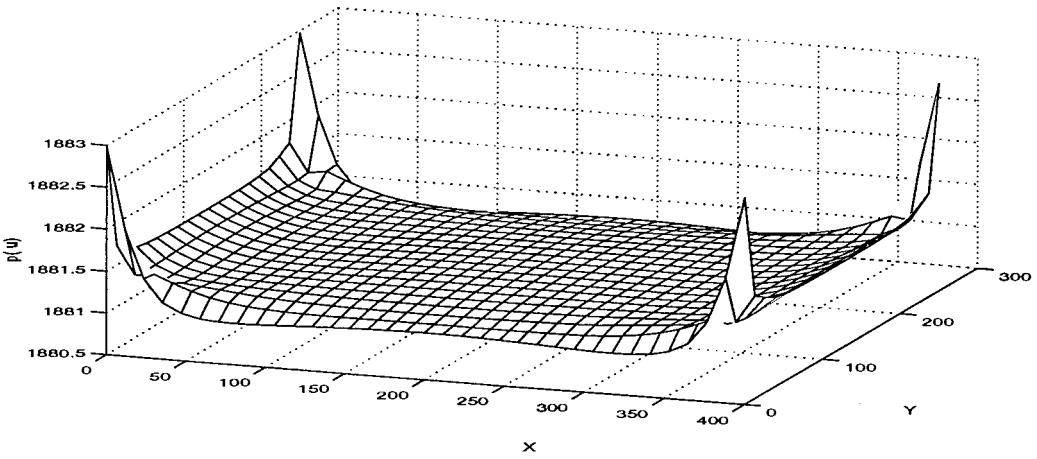

Figure 5. Computed warp/weft contact pressure of the plate Ω subjected to a prescribed displacement $u^{\alpha}_{\Gamma_1} = 5\mathbf{e_1}$ mm.

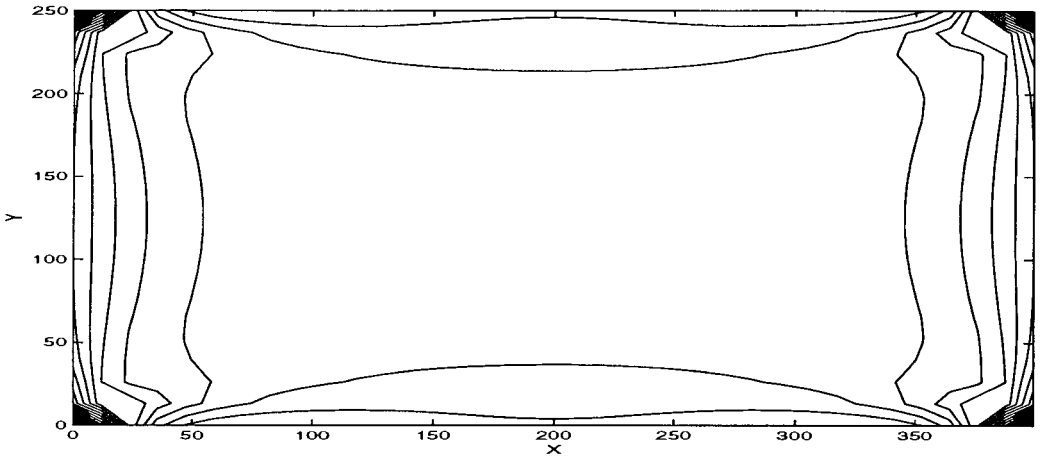

Figure 6. Computed warp/weft contact pressure contour of the plate Ω subjected to a prescribed displacement $u^{\alpha}_{\Gamma_1} = 5\mathbf{e_1}$ mm.

The product space $\mathbf{H^1}(\Omega)$ is a Hilbert space equipped with the inner product and associated norm

$$(\mathbf{u}, \mathbf{v})_{\mathbf{1}} = \int_{\Omega} \left(u_i^{\alpha} v_i^{\alpha} + \partial_j u_i^{\alpha} \partial_j v_i^{\alpha} \right) \mathrm{d}x \quad \text{and} \quad \|\mathbf{v}\|_1 = [(\mathbf{v}, \mathbf{v})_{\mathbf{1}}]^{1/2}.$$

We introduce the following notations

$$a(\mathbf{u}, \mathbf{v}) = \int_{\Omega} \sigma_{ij}^{\alpha}(u^{\alpha}) \mathcal{E}_{ij}(v^{\alpha}) \mathrm{d}x = a^{\alpha}(u^{\alpha}, v^{\alpha}), \tag{14}$$

$$\tilde{f}(\mathbf{v}) = \int_{\Omega} f^{\alpha} \cdot v^{\alpha} \mathrm{d}x = \tilde{f}^{\alpha}(v^{\alpha}), \tag{15}$$

with usual assumptions on (a^{α}_{ijkl}) and f^{α}.

We introduce the following nonlinear functional Φ, which serves to characterize the virtual work of frictional forces

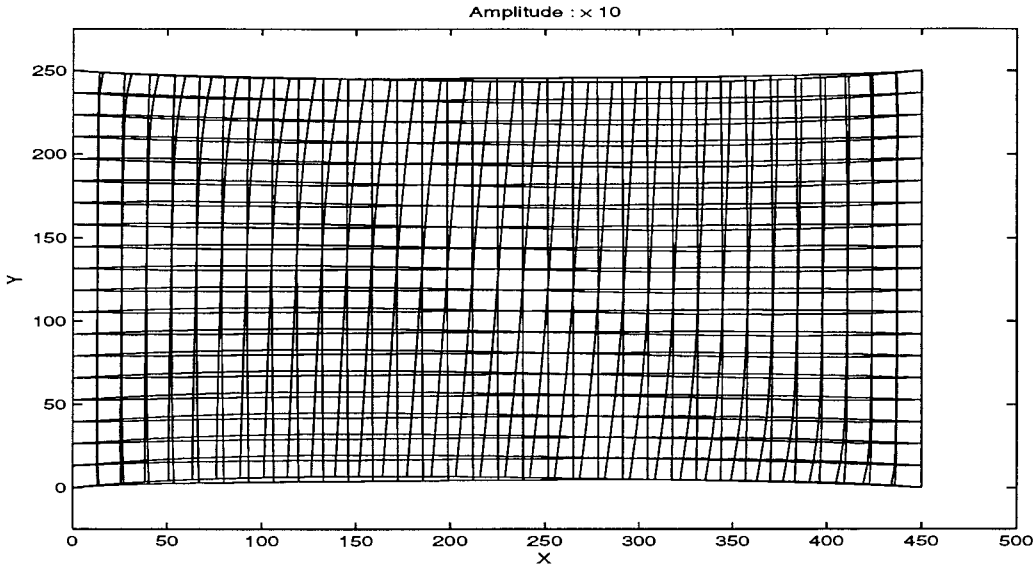

Figure 7. Deformed configuration of the plate Ω subjected to a prescribed displacement $u^{\alpha}_{\Gamma_1} = 5\mathbf{e_1}$ mm, with orthotropic axes orientation $\theta = 30°$.

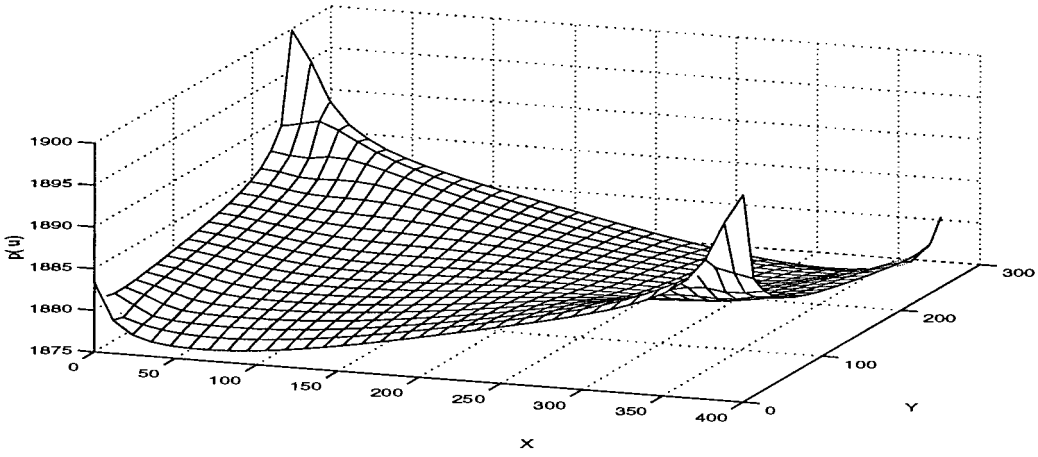

Figure 8. Computed warp/weft contact pressure of the plate Ω subjected to a prescribed displacement $u^{\alpha}_{\Gamma_1} = 5\mathbf{e_1}$ mm, with orthotropic axes orientation $\theta = 30°$.

$$\Phi(\mathbf{u}, \mathbf{v}) = \int_{\Omega} p(\mathbf{u})|\bar{\mathbf{v}}|\mathrm{d}x, \tag{16}$$

where $\bar{\mathbf{v}} = v^1 - v^2$ is the virtual relative tangential displacement and $p(\mathbf{u})$ the warp/weft contact pressure given by (13). The functional Φ is well defined for $\mathbf{u}, \mathbf{v} \in \mathbf{H^1}(\Omega)$.

Finally, the set of admissible displacement fields is given by

$$\mathbf{K} = \{\mathbf{v} = (v^1, v^2) \in \mathbf{H^1}(\Omega)|\mathbf{v} = 0 \quad \text{on } \Gamma_0\} = K^1 \times K^2, \tag{17}$$

where

$$K^{\alpha} = \{v^{\alpha} \in (H^1(\Omega))^2|v^{\alpha} = 0, \quad \text{on } \Gamma_0^{\alpha}\}.$$

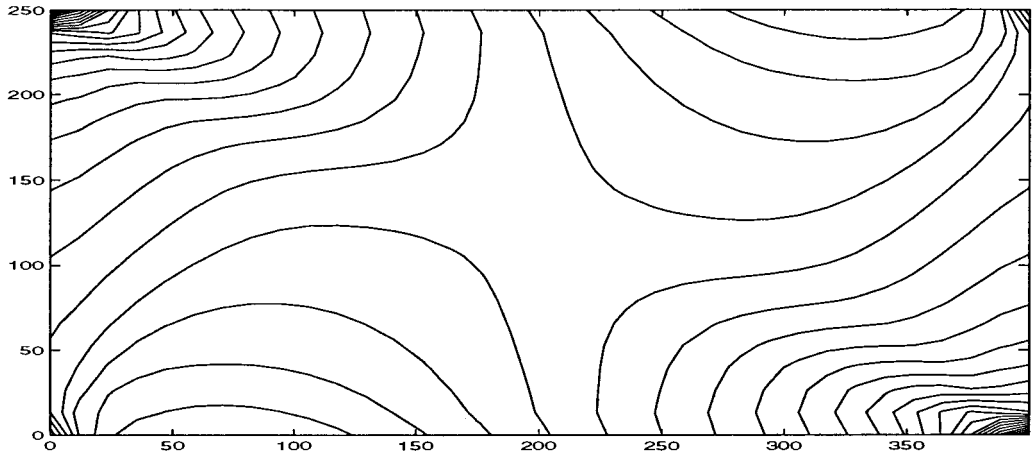

Figure 9. Computed warp/weft contact pressure contour of the plate Ω subjected-to-a prescribed displacement $u^{\alpha}_{\Gamma_1} = 5\mathbf{e_1}$ mm, with orthotropic axes orientation $\theta = 30°$.

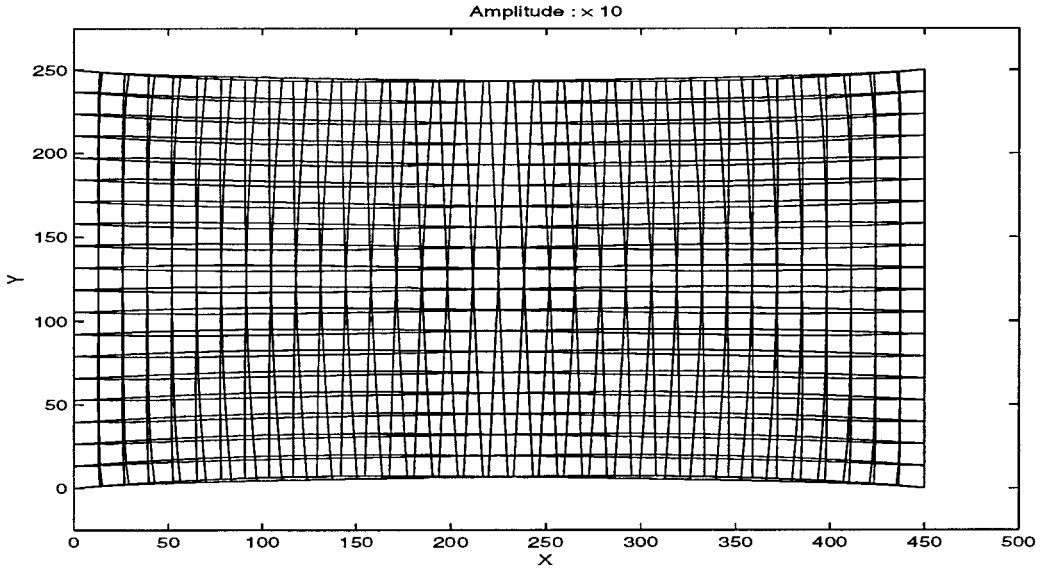

Figure 10. Deformed configuration of the plate Ω subjected to a prescribed displacement $u^{\alpha} = 5\mathbf{e_1}$ mm, with orthotropic axes orientation $\theta = 45°$.

The variational principle for problem (5) - (8) is established through the following theorem.

Theorem 1 *A displacement field* $\mathbf{u} = (u^1, u^2)$ *is a solution to (5) - (8), if* $\mathbf{u}$ *satisfies*

$$\mathbf{u} \in \mathbf{K}, a(\mathbf{u}, \mathbf{v} - \mathbf{u}) + \mu_F \Phi(\mathbf{u}, \mathbf{v}) - \mu_F \Phi(\mathbf{u}, \mathbf{u}) \geq \tilde{f}(\mathbf{v} - \mathbf{u}), \quad \forall \mathbf{v} \in \mathbf{K}. \tag{18}$$

The proof of the theorem 1 is almost the same as the proof of [7, theorem 10.1] with $\mathbf{u}_T = \bar{\mathbf{u}}$, $\mathbf{u}_n = 0$ and $\sigma_n(\mathbf{u}) = p(\mathbf{u})$.

5. Numerical approximation

The crucial point of the variational inequality (18) is that the friction term Φ is non convex and non differentiable. These properties are particularly troublesome when one attempts to

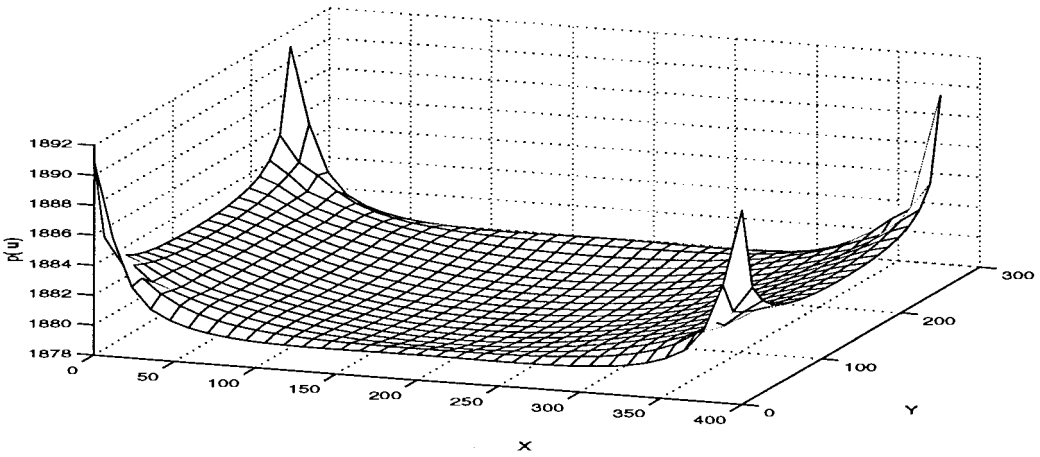

Figure 11. Computed warp/weft contact pressure of the plate Ω subjected to a prescribed displacement $u^{\alpha}_{\Gamma_1} = 5\mathbf{e_1}$ mm with orthotropic axes orientation $\theta = 45°$.

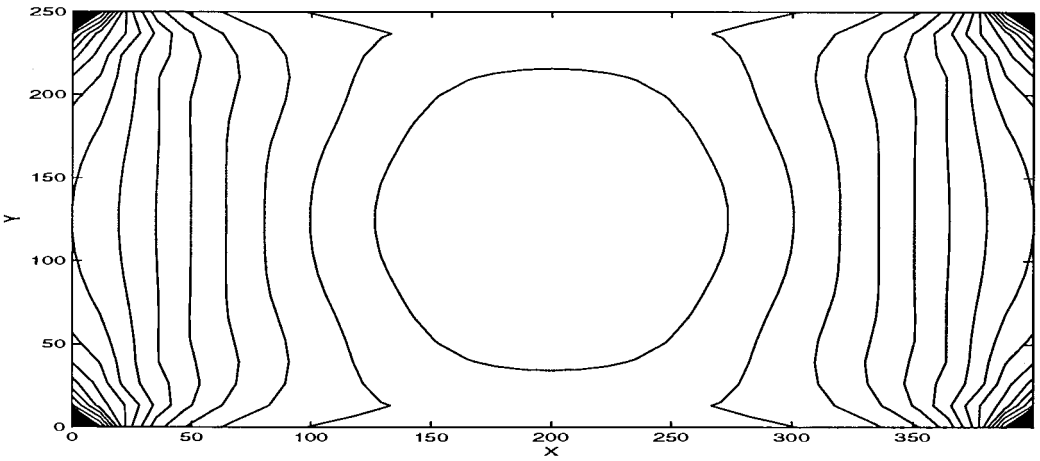

Figure 12. Computed warp/weft contact pressure contour of the plate Ω subjected to a prescribed displacement $u^{\alpha}_{\Gamma_1} = 5\mathbf{e_1}$ mm, with orthotropic axes orientation $\theta = 45°$.

develop numerical methods for solving (18). To overcome these difficulties, a classical way in nonlinear mechanics is to work in two steps: first a reduced problem, in which the contact pressure $p(\mathbf{u})$ is assumed to be known, is solved; and second, an iterative scheme for solving the general inequality (18) is constructed.

5.1. THE REDUCED PROBLEM

We assume that the contact pressure, $p = p(x_1, x_2)$, is known. Then the friction term (16) becomes

$$\Phi(\mathbf{v}) = \int_{\Omega} p|\bar{\mathbf{v}}|\mathrm{d}x. \tag{19}$$

The functional $\Phi(\mathbf{v})$ is still non-differentiable, but it is now convex and lower semi-continuous. The variational inequality (18) is now reduces to

$$\mathbf{u} \in \mathbf{K}, a(\mathbf{u}, \mathbf{v} - \mathbf{u}) + \mu_F \Phi(\mathbf{v}) - \mu_F \Phi(\mathbf{u}) \geq \tilde{f}(\mathbf{v} - \mathbf{u}), \quad \forall \mathbf{v} \in \mathbf{K}. \tag{20}$$

To overcome the non-differentiability of Φ, a classical way is to use a regularization of the Euclidean norm $|\cdot|$ in (19). We can use, for example, the following regularization function

$$\rho_\varepsilon : \mathbb{R}^2 \longrightarrow \mathbb{R}; \quad \rho_\varepsilon(x) = \begin{cases} |x| - \varepsilon/2, & \text{if } |x| > \varepsilon, \\ |x|^2/(2\varepsilon), & \text{if } |x| \leq \varepsilon, \end{cases}$$

where ε is a small positive number (the regularization parameter). Then the regularized functional Φ_ε of Φ is given by

$$\Phi_\varepsilon(\mathbf{v}) = \int_\Omega p\rho_\varepsilon(\bar{\mathbf{v}})\mathrm{d}x. \tag{21}$$

The functional Φ_ε is Gâteaux differentiable, with

$$\langle D\Phi_\varepsilon(\mathbf{u}_\varepsilon, \mathbf{v}\rangle, = \int_\Omega \frac{\partial \rho_\varepsilon}{\partial \mathbf{u}}(\bar{\mathbf{u}}) \cdot \bar{\mathbf{v}}\, \mathrm{d}x,$$

where

$$\frac{\partial \rho_\varepsilon}{\partial \mathbf{u}}(\bar{\mathbf{u}}) = \begin{cases} \bar{\mathbf{u}}/|\bar{\mathbf{u}}| & \text{if } |\bar{\mathbf{u}}| > \varepsilon \\ \bar{\mathbf{u}}/\varepsilon & \text{if } |\bar{\mathbf{u}}| \leq \varepsilon. \end{cases}$$

The corresponding variational inequality is then

$$\mathbf{u}_\varepsilon \in \mathbf{K}, \quad a(\mathbf{u}_\varepsilon, \mathbf{v} - \mathbf{u}_\varepsilon) + \mu_F \Phi_\varepsilon(\mathbf{v}) - \mu_F \Phi(\mathbf{u}_\varepsilon) \geq \tilde{f}(\mathbf{v} - \mathbf{u}_\varepsilon), \quad \forall \mathbf{v} \in \mathbf{K}. \tag{22}$$

Since Φ_ε is convex, (22) is a convex minimization problem. It follows that a solution $\mathbf{u}_\varepsilon$, of (22) is a solution of the variational equality

$$\mathbf{u}_\varepsilon \in \mathbf{K}, \quad a(\mathbf{u}_\varepsilon, \mathbf{v}) + \mu_F \langle D\Phi_\varepsilon(\mathbf{u}_\varepsilon), \mathbf{v}\rangle = \tilde{f}(\mathbf{v}), \quad \forall \mathbf{v} \in \mathbf{K}. \tag{23}$$

The discretization of (23) is obtained in the usual way. Let $\Omega_h = \cup_e \Omega_e(h), h > 0$, be a regular triangulation of Ω. We note $\mathbf{u}_h = (u_h^1, u_h^2)$ a finite-dimensional approximation of $\mathbf{u}$ over Ω_h and $\mathbf{K}_h$ a finite-dimensional subset of $\mathbf{K}$. The finite elements approximation of the variational equality (23) is

$$\mathbf{u}_{\varepsilon h} \in \mathbf{K}_h, \quad a(\mathbf{u}_{\varepsilon h}, \mathbf{v}_h) + \mu_F \langle D\Phi_\varepsilon(\mathbf{u}_{\varepsilon h}), \mathbf{v}_h\rangle = \tilde{f}(\mathbf{v}_h), \quad \forall \mathbf{v}_h \in \mathbf{K}_h. \tag{24}$$

Equation (24) leads to a nonlinear system which can be solved by a standard Newton-Raphson method or a successive iterative method. In this last method, at the kth iteration, we solve the linear system in $\mathbf{u}_{\varepsilon h}^k$

$$a(\mathbf{u}_{\varepsilon h}^k, \mathbf{v}_h) + \mu_F \langle (D\Phi_\varepsilon(\mathbf{u}_{\varepsilon h}^{k-1}), \mathbf{v}_h\rangle = \tilde{f}(\mathbf{v}_h), \quad \forall \mathbf{v}_h \in \mathbf{K}_h, \tag{25}$$

for $k = 1, 2, 3, \ldots$, for an initial approximation $\mathbf{u}_{\varepsilon h}^0$.

We can now define the approximation of the full adhesion zones and the sliding zones. For this purpose, we set

$|\bar{\mathbf{u}}_{\varepsilon h}| < \varepsilon \implies$ full adhesion,

$|\bar{\mathbf{u}}_{\varepsilon h}| \geq \varepsilon \implies$ sliding.

5.2. THE GENERAL PROBLEM

The extension of the previous results to the general variational inequality (18) is straightforward. We simply use an iterative method for approximating the contact pressure $p(\mathbf{u})$. Indeed, at the kth iteration, we use in the formula (19) $p^k = p(\mathbf{u}_{\varepsilon h}^{k-1})$, *i.e.* the contact pressure obtained at the end of the previous step. The process is repeated until successive contact pressures do not differ by a preassign tolerance ε_p, *i.e.* $\|p^k - p^{k-1}\|/\|p^k\| < \varepsilon_p$.

With the above calculations, the practical implementation of the numerical method for solving (18) can finally be described as follows.

Step 0. Initialization. $k \leftarrow 0$, $\mathbf{u}_{\varepsilon h}^0 = 0$ (full adhesion), $p^1 = p(\mathbf{u}_{\varepsilon h}^0)$

Step 1. $k \leftarrow k+1$ Solve the nonlinear system in $\mathbf{u}_{\varepsilon h}^k$ (24). Compute the new contact pressure $p^{k+1} = p(\mathbf{u}_{\varepsilon h}^k)$.

Step 2. If $\|p^{k+1} - p^k\|/\|p^{k+1}\| < \varepsilon_p$ then STOP else go to Step 1.

In all the examples reported in the next section, the algorithm stopped with $k \leq 5$. In Step 2, we use the successive iterative scheme (25) for computing $\mathbf{u}_{\varepsilon h}^k$ for obvious simplicity reasons. Furthermore, it provides very rapid convergence if $\mathbf{u}_{\varepsilon h}^{k-1}$ is used as an initial approximation when computing $\mathbf{u}_{\varepsilon h}^k$.

5.3. NUMERICAL EXPERIMENTS

The numerical algorithm described in the previous section was implemented in Fortran 77 on a SGI Octane workstation, with the regularization parameter $\varepsilon = 10^{-5}$ and the contact pressure tolerance $\varepsilon_p = 10^{-5}$.

We consider the textile composite plate Ω, represented in Figure 3, made from flat glass fibers. The composite plate is fixed on its left boundary $\Gamma_0 = \{x = 0\}$, *i.e.* $\mathbf{u}_{\Gamma_0} = 0$. The upper boundary ($y = 250$) and the lower boundary ($y = 0$) are free. Note that the final goal of our study is the modeling of the forming of textile composite plates. Since the forming is a prescribed-displacements process, the numerical examples presented here deal with a prescribed displacements on Γ_1.

The weaving introduces an initial contact pressure $\eta = 1870$ MPa. The friction coefficient of glass fibers is $\mu_F = 0{\cdot}3$. The homogenized elastic moduli of each layer of the plate are:

$$E_L^1 = 13800 \text{ MPa}, E_T^1 = 5200 \text{ MPa}, \nu_{LT}^1 = 0{\cdot}12, G_{LT}^1 = 1870 \text{ MPa},$$

$$E_L^2 = 5200 \text{ MPa}, E_T^2 = 13800 \text{ MPa}, \nu_{LT}^2 = 0{\cdot}12, G_{LT}^2 = 1870 \text{ MPa},$$

with E_L the longitudinal Young's modulus, E_T the transverse Young's modulus, ν_{LT} the Poisson's ratio and G_{LT} the shear modulus. The thickness of each layer of the plate is $e = 0{\cdot}7$ mm.

The weaving is characterized by a wavelength $l^\alpha = 10$ mm, $\alpha = 1, 2$, and an amplitude $d^\alpha = 0{\cdot}7$ mm, $\alpha = 1, 2$. With the data above, the reduction factor in (4) is $\kappa^\alpha = 0{\cdot}812248$, $\alpha = 1, 2$.

A finite-element mesh, of the plate, consisting of 646 4-nodes isoparametric elements (700 nodes) for Ω^α, for $\alpha = 1, 2$, is represented in Figure 3. The meshes of the two layers coincide in the undeformed configuration of the plate. Since we consider the plate as an assembly of two continuous layers, the mesh of the plate does not necessary coincide with the natural mesh of the textile composite.

In the first example, we study the behavior of the model in the case of a prescribed displacement $u_{\Gamma_1}^\alpha = 5\mathbf{e_1}$ mm, for $\alpha = 1, 2$, with $\mathbf{e_1}$ the first natural base vector of $\mathbb{R}^2$. Figure 4

represents the computed deformed configuration of the textile composite plate. The sliding zones are represented by duplicated lines. The resulting contact pressure is represented in Figure 5–6. Note that there is no sliding where the contact pressure is higher, *i.e.* near the boundaries Γ_0 and Γ_1. The variation of the contact pressure $p(\mathbf{u})$ observed is significant.

We now study the case the orthotropic axes of the plate do not coincide with co-ordinates axes,(*i.e.* the orientation of the fibers do not coincides with natural base vectors $\mathbf{e_1}$ and $\mathbf{e_2}$). If the x_1-fibers orientation is obtained by a rotation θ with respect to the x_1-axis, then the elastic moduli tensor (4) becomes (repeated index convention)

$$a^{\alpha}_{ijkl} = \kappa^{\alpha}\tilde{a}^{\alpha}_{IJKL}\mathcal{R}_{Ii}\mathcal{R}_{Jj}\mathcal{R}_{Kk}\mathcal{R}_{Ll},$$

where $\mathcal{R}$ is the rotation matrix

$$\mathcal{R} = \begin{pmatrix} \cos\theta & -\sin\theta \\ \sin\theta & \cos\theta \end{pmatrix}.$$

Note that we need the strain tensor components $\mathcal{E}_{11}(u^1) = \partial_1 u^1_1$ and $_{22}(u^2) = \partial_2 u^2_2$ in the warp/weft contact pressure formula (13). If we set $\mathcal{E}'(u^\alpha) = \mathcal{R}^{-1}\mathcal{E}(u^\alpha)\mathcal{R}$, then in (13) we must use $\mathcal{E}'_{11}(u^1)$ and $\mathcal{E}'_{22}(u^2)$.

The computed deformed shape of mesh and the contact pressure distribution are summarized in Figures 7–9, for $\theta = 30°$, and Figures 10–12, for $\theta = 45°$. Since the plate is more deformable, the computed sliding zones observed in Figure 7 and Figure 10 are significant. As for $\theta = 0°$, there is no sliding in high contact pressure zones.

6. Conclusion

We have studied a new mathematical model of textile composite plates with warp/weft frictional contact. Numerical experiments show that the slippage of warp and weft fibers relative to one another occurs within the plate. Numerical experiments also show that the variation of the warp/weft contact pressure contributes to maintaining the cohesion of the plate.

Homogenization techniques used in the model allowed us to use meshes which do not necessarily coincide with the natural mesh of the textile composite plate. That is a significant advantage over geometrical models when dealing with wide textile composite plate.

The angular variation ϕ of the warp and weft directions can be computed. Let ϕ_1 and ϕ_2 be the angular variations of the warp and weft directions with respect to $\mathbf{e_1}$. For $\theta = 0$, for example, we have $\cos\phi_1 = u^1_1/|u^1|$ and $\cos\phi_2 = u^2_2/|u^2|$; and $\phi = \phi_2 - \phi_1$. Note that the feasibility of a forming is restricted by the angular variation.

Current study is directed towards extending the model to the forming of textile composite plates. For this purpose, we will consider the complete Saint-Venant-Kirchoff strain tensor, *i.e.*

$$\mathcal{E}_{ij}(u^\alpha) = \frac{1}{2}(\partial_i u^\alpha_j + \partial_j u^\alpha_i + \partial_i u^\alpha_k \partial_j u^\alpha_k)$$

and the complete stretch formula (11) in the warp/weft contact pressure formula (10). A quasi-static scheme will be introduced to overcome the strong nonlinearities. Then at each step of the quasi-static scheme, the results of this study could be used.

References

1. B.N. Cox and G. Flanagan, *Handbook of Analytical Methods for Textiles Composites*. Langley Research Center: NASA Contractor Report 4750 (1997) 162 pp.
2. D. Caillerie and H. Tollenaère, Modèles bidimensionals de tissés. *Comptes Rendus de l'Acad. des Sc. Paris* 318 I (1994) 87–92.
3. F. Lené and D. Leguillon, Etude de l'influence du glissement entre les constituants d'un matériau composite sur ses coefficients effectifs. *J. de Mécanique* 20 (1981) 509–536.
4. F. Bendali, J. Koko and A. Quilliot, Draping of fabrics over arbitrary surfaces: an augmented Lagrangian method. *J. Textile Inst.* 90 (1999) 177–186.
5. B.P. Van West, R.B. Pipes and M. Keefe, A simulation of the draping of bidirectional fabrics over arbitrary surfaces. *J. Textile Inst.* 81 (1990) 448–460.
6. B.N. Cox and M.S. Dadkhah, The macroscopic elasticity of 3D woven composites. *J. Composite Materials* 29 (1995) 785–819.
7. N. Kikuchi and J.T. Oden, *Contact Problems in Elasticity*. Philadelphia: SIAM Studies 8 (1988) 495 pp.